

# Modulation of Intracellular Ceramide Using Polymeric Nanoparticles to Overcome Multidrug Resistance in Cancer

Lilian E. van Vlerken,<sup>1</sup> Zhenfeng Duan,<sup>2</sup> Michael V. Seiden,<sup>2</sup> and Mansoor M. Amiji<sup>1</sup>

<sup>1</sup>Department of Pharmaceutical Sciences, School of Pharmacy, Northeastern University and <sup>2</sup>Department of Hematology and Oncology, Massachusetts General Hospital, Boston, Massachusetts

## Abstract

Although multidrug resistance (MDR) is known to develop through a variety of molecular mechanisms within the tumor cell, many tend to converge toward the alteration of apoptotic signaling. The enzyme glucosylceramide synthase (GCS), responsible for bioactivation of the proapoptotic mediator ceramide to a nonfunctional moiety glucosylceramide, is overexpressed in many MDR tumor types and has been implicated in cell survival in the presence of chemotherapy. The purpose of this study was to investigate the therapeutic strategy of coadministering ceramide with paclitaxel, a commonly used chemotherapeutic agent, in an attempt to restore apoptotic signaling and overcome MDR in the human ovarian cancer cell line SKOV3. Poly(ethylene oxide)-modified poly(epsilon-caprolactone) (PEO-PCL) nanoparticles were used to encapsulate and deliver the therapeutic agents for enhanced efficacy. Results show that indeed the cotherapy eradicates the complete population of MDR cancer cells when they are treated at their IC<sub>50</sub> dose of paclitaxel. More interestingly, when the cotherapy was combined with the properties of nanoparticle drug delivery, the MDR cells can be resensitized to a dose of paclitaxel near the IC<sub>50</sub> of non-MDR (drug sensitive) cells, indicating a 100-fold increase in chemosensitization via this approach. Molecular analysis of activity verified the hypothesis that the efficacy of this therapeutic approach is indeed due to a restoration in apoptotic signaling, although the beneficial properties of PEO-PCL nanoparticle delivery seemed to enhance the therapeutic success even further, showing the promising potential for the clinical use of this therapeutic strategy to overcome MDR. [Cancer Res 2007;67(10):4843–50]

## Introduction

A major clinical obstacle in cancer therapy is the development of resistance to a multitude of chemotherapeutic agents, a phenomenon termed multidrug resistance (MDR). The development of drug resistance in a small subset of tumor cells is believed to be the cause for tumor survival despite invasive chemotherapy (1), a burden particularly in the treatment of ovarian cancer, in which MDR occurs in at least 50% of patients upon relapse (2). Cancer cells can acquire MDR through several molecular mechanisms, in which often more than one mechanism may be responsible for the MDR phenotype (1, 3). These common causes for MDR include overexpression of membrane spanning ATP-dependent

drug efflux pumps from the ABC transporter family (most notably P-glycoprotein/MDR-1), modifications in drug metabolism through glutathione-S-transferase or cytochrome P450 activity, alterations in DNA repair mechanisms, and modifications of apoptotic signaling (1, 3).

Another major barrier to successful anticancer therapy is the challenge of delivering the required therapeutic concentration to the tumor site while minimizing undesirable side effects resulting from systemic administration. Site-specific drug delivery systems increase the therapeutic benefit by delivering a greater fraction of the dose at the target site which minimizes the amount of therapeutic that accumulates at nonspecific targets. Biodegradable polymeric nanoparticles, such as poly(epsilon-caprolactone) (PCL), are useful drug delivery carriers for such tumor targeted delivery (4, 5). Biocompatibility and degradation methods of this polymer have been widely studied (6–8) and found to be nontoxic, leading to the U.S. Food and Drug Administration approval and acceptance of PCL for medical applications. Additionally, PCL offers an advantage for drug delivery whereby its alkyl structure efficiently encapsulates hydrophobic compounds, whereas slow degradation of the particle allows for extended release of the drug (9). Surface modification of the nanoparticles with a poly(ethylene oxide)-poly(propylene oxide) triblock copolymer (PEO-PPO-PEO, Pluronic) improves the stability of the nanoparticle in the aqueous environment of the body, while decreasing immune activation, repelling plasma proteins, and decreasing reticuloendothelial uptake leading to an increase in circulation time (10). PEO-modified nanoparticles also preferentially localize in the tumor mass by the enhanced permeability and retention effect (11), whereby the fenestrated tumor interstitium and poor lymphatic drainage cause the nanoparticles to extravasate and deliver their drug load. Previous studies from our group have shown that paclitaxel-containing poly(ethylene oxide)-modified poly(epsilon-caprolactone) (PEO-PCL) nanoparticles remain stable *in vivo* and retain their Pluronic surface layer to increase the circulating half-life and plasma residence time of paclitaxel from a fraction of an hour to 25.3 and 24.0 h, respectively, alongside a nearly 8-fold decrease in total body clearance of the drug (10, 12). The concentration of paclitaxel inside the tumor mass of mice-bearing human ovarian carcinoma (SKOV3) xenografts, as a result, was 8.7-fold higher at 5 h postinjection compared with mice treated with paclitaxel solution (12).

Paclitaxel, an antitumor chemotherapeutic agent originally derived from the bark of the Pacific yew tree (*Taxus brevifolia*; ref. 13), is widely used in the treatment of solid tumors, particularly of the breast and ovaries (14). Paclitaxel exerts its cytotoxicity by inducing tubulin polymerization resulting in unstable microtubules which interferes with mitotic spindle function and ultimately arrests cells in the G<sub>2</sub>-M phase of mitosis (15, 16). Although it is understood that cell cycle arrest results in activation of the apoptotic signaling cascade, recent studies suggest that paclitaxel

**Requests for reprints:** Mansoor M. Amiji, 110 Mugar Life Sciences Building, 360 Huntington Avenue, Boston, MA 02115. Phone: 617-373-3137; Fax: 617-373-8886; E-mail: m.amiji@neu.edu.

©2007 American Association for Cancer Research.  
doi:10.1158/0008-5472.CAN-06-1648

therapy specifically results in accumulation of endogenous ceramide, a lipid with function as a cellular second messenger in apoptosis (17).

Ceramide, a naturally occurring sphingolipid, is derived intracellularly by hydrolysis of the lipid sphingomyelin or by *de novo* synthesis through N-acylation of sphinganine (18). Accumulation of endogenous ceramide produced by either hydrolysis or *de novo* formation is known to result in response to several stimuli, such as growth factor deprivation, proinflammatory signals, exposure to increased temperature and radiation, and other stressors, such as chemotherapeutics and related cytotoxic agents (18, 19). Among such stimuli, paclitaxel has been shown to elevate intracellular ceramide levels in breast cancer cells (17). Intracellular ceramide is implicated in the cellular responses to stress, such as apoptosis and cell cycle arrest (17, 20–22), in which ceramide functions as a second messenger in the signaling cascade that initiates these responses. In fact, studies have shown that administration of exogenous ceramide analogues, particularly C<sub>2</sub>-ceramide and C<sub>6</sub>-ceramide, encourages cell death by apoptosis and inhibition of tumor growth in several tumor models (20, 21, 23–25). In the cell, ceramide can subsequently be further metabolized by the enzyme glucosylceramide synthase (GCS) to yield glucosylceramide, a glycosylated form of ceramide that does not have proapoptotic activity (26–30). Several MDR tumor cell lines have exhibited elevated levels of noncytotoxic glucosylceramide and corresponding elevated levels of GCS (26–30), and clinical studies have noted elevation of glucosylceramide levels in tumor specimens of breast cancer and melanomas that were poorly responsive to chemotherapy (29). These findings not only suggest the importance of ceramide in the mediation of the cytotoxic response to antitumor chemotherapeutics, but they also suggest that inhibition of apoptotic signaling may be an important mechanism whereby tumors develop MDR.

The purpose of this study was to overcome the cellular mechanisms of MDR through a therapeutic strategy that would overcome the obstruction to apoptotic signaling, thereby resensitizing the MDR cancer cells to chemotherapy. This novel therapeutic strategy entails the coadministration of the chemotherapeutic drug paclitaxel with the apoptosis modulator ceramide, encapsulated within PEO-PCL nanoparticles for optimal therapeutic efficacy. In this manner, we hypothesize that exogenous ceramide administration renders unmetabolized ceramide available in the cell to reinstate apoptotic signaling resulting from paclitaxel exposure.

## Materials and Methods

**Preparation and characterization of PEO-PCL nanoparticles.** Drug-containing-PEO-PCL nanoparticles were prepared as previously described by controlled solvent displacement method using an acetone-water system (10). Paclitaxel and tamoxifen (ICN), *N*-hexanoyl-D-erythrospingosine (C<sub>6</sub>-ceramide, Avanti Polar Lipids), and verapamil HCl (Sigma-Aldrich) were independently encapsulated into PEO-PCL nanoparticles at 10% (w/w) for paclitaxel or 20% (w/w) for ceramide, tamoxifen, and verapamil. Nanoparticles were characterized on a Brookhaven ZetaPlus particle analyzer (Brookhaven Instruments) and by scanning electron microscopy (SEM) on a Hitachi S-4800 instrument.

Drug release studies were done in PBS with 0.1% Tween-80 at either pH 7.4 or pH 6.5 at 37°C for up to 5 days. At daily intervals, samples of release medium were collected, and the exact volume of release buffer taken was replaced to maintain sink conditions. Paclitaxel release was measured by reverse-phase high-performance liquid chromatography on a C18 column with 50/50 acetonitrile-sodium phosphate buffer containing 20 mmol/L

SDS. Ceramide release was measured by incorporating 1% (w/w) NBD-ceramide into the nanoparticles and monitoring the NBD-ceramide fluorescence on a plate reader at 485/530 nm excitation/emission.

**Cell culture and treatment.** Wild-type (drug sensitive) SKOV3 and SKOV3TR (MDR) human ovarian carcinoma cells (kindly provided by Dr. Michael Seiden, Massachusetts General Hospital) were maintained in fetal bovine serum (FBS)-supplemented RPMI-1640 (Mediatech, Inc.), whereby the SKOV3<sub>TR</sub> subculture was selected and maintained for MDR by the addition of 0.2 μmol/L paclitaxel in the culture medium. Acute myelogenous leukemia (AML)-12 murine hepatocytes (American Type Culture Collection) were maintained in FBS-supplemented DMEM (Mediatech). For experiments, cells were plated at 5,000 cells per well and subjected to treatment with various doses of the investigational compounds as free drugs or encapsulated in PEO-PCL nanoparticles diluted in supplemented medium. The pan-caspase inhibitor ZVAD.fmk was obtained from Axxora. In all studies, treatment with vehicles was included for control purposes. Treatment with serum-supplemented medium was used as a negative control (0% cell death), and treatment with 50 μg/mL poly(ethyleneimine) (molecular weight, 10 kDa) was used as a positive control (100% cell death). Treatment proceeded undisturbed for 6 days, after which cell viability was measured by the MTS assay.

**Protein extraction and Western blotting.** Protein was extracted from basal or drug-treated cells and separated on a 4% to 15% SDS-PAGE gradient gel (Bio-Rad) and transferred on to nitrocellulose membrane. Blots were incubated with anti-P-glycoprotein monoclonal antibody C219 (Signet Labs), anti-GCS polyclonal antibody (Exalpa Biochemicals), anti-caspase-3 monoclonal antibody (Cell Signaling Tech.), or anti-β-actin monoclonal antibody (Cell Signaling Tech.) for 16 h at 4°C, followed by a 1.5-h incubation at room temperature with a horseradish peroxidase-conjugated secondary antibody (Cell Signaling Tech.). To visualize the proteins of interest, the membrane was incubated for 3 min in enhanced chemiluminescence substrate (Pierce) according to protocol and exposed to film.

**Measurement of intracellular drug uptake.** Drug-loaded PEO-PCL nanoparticles were manufactured as previously described, with the addition of [<sup>3</sup>H]paclitaxel (Moravak Biochemicals) and [<sup>14</sup>C]ceramide (American Radiolabeled Chemicals) at 1.5 μCi/mg unlabeled drug. Cells were seeded at 100,000 cells per well and treated with varying doses of the combination therapy for 6 h at 37°C. Subsequently, cells were washed twice with PBS, lysed with 1 mL of lysis buffer, and collected in scintillation vials. Each sample received 10 mL Scintisafe scintillation fluid (Fisher Scientific) and was left to quench for 2 h in the dark before scintillation counting. For parallel experiments, rhodamine-123 was encapsulated into PEO-PCL nanoparticles at 1% w/w as previously described. Cells were allowed to adhere on flame-sterilized glass coverslips and incubated with 10 μg rhodamine-123 given as free compound or within nanoparticles for 4 h. Cells were washed thrice with PBS, and coverslips mounted onto glass slides with Fluoromount-G fixing medium (SBA). Images were obtained on an Olympus BX61W1 fluorescence microscope using a 546/590 excitation/emission filter maintaining an exposure time of 400 ms. All treatments were triplicated.

**Fluorescence-labeled nanoparticle trafficking.** PEO-PCL nanoparticles containing rhodamine-paclitaxel (Boston Scientific Corporation) and NBD-ceramide (Molecular Probes) were manufactured as previously described loaded at 0.1% (w/w). Cells were plated onto glass coverslips and incubated with a 0.1 μmol/L solution of rhodamine-paclitaxel and NBD-ceramide nanoparticles for 6 h. Cells were washed, coverslips were fixed onto slides with Fluoromount-G medium, and images were obtained on an Olympus BX61W1 fluorescence microscope using 546/590 and 485/530 filters for rhodamine and NBD signals, respectively. All treatments were duplicated.

**Analysis of apoptotic activity.** Cells were collected and counted as previously described, subsequently plated in 96-well optical quality plates (Nalge-Nunc, Int.), and treated with paclitaxel and/or ceramide for 12 or 24 h alongside control treatment (medium). After treatment, cells were stained for apoptosis with Yo-Pro-1, propidium iodide, and Hoechst-33342 (Vybrant apoptosis assay kit 7, Molecular Probes) and analyzed by *in-situ* cytometric analysis of live cells using the iCys microplate cytometry platform (Compucyte Corp.) Yo-Pro and propidium iodide were excited at 488 nm absorbed at 515 to 545 nm and 600 to 635 nm, respectively, whereas Hoechst

was excited at 405 nm and absorbed at 445 to 485 nm. Each sample scan was repeated four times, all treatments were run in triplicate, and the entire set up and analysis was repeated once more at a later date.

**Statistical analysis.** For the cytotoxicity experiments,  $n = 8$  measurements per treatment, whereas for the apoptosis assay,  $n = 6$  measurements per treatment were used. Statistical analysis was done by two-tailed, equal variance Student's  $t$  test. Results were considered significant at 95% confidence interval (i.e.,  $P < 0.05$ ).

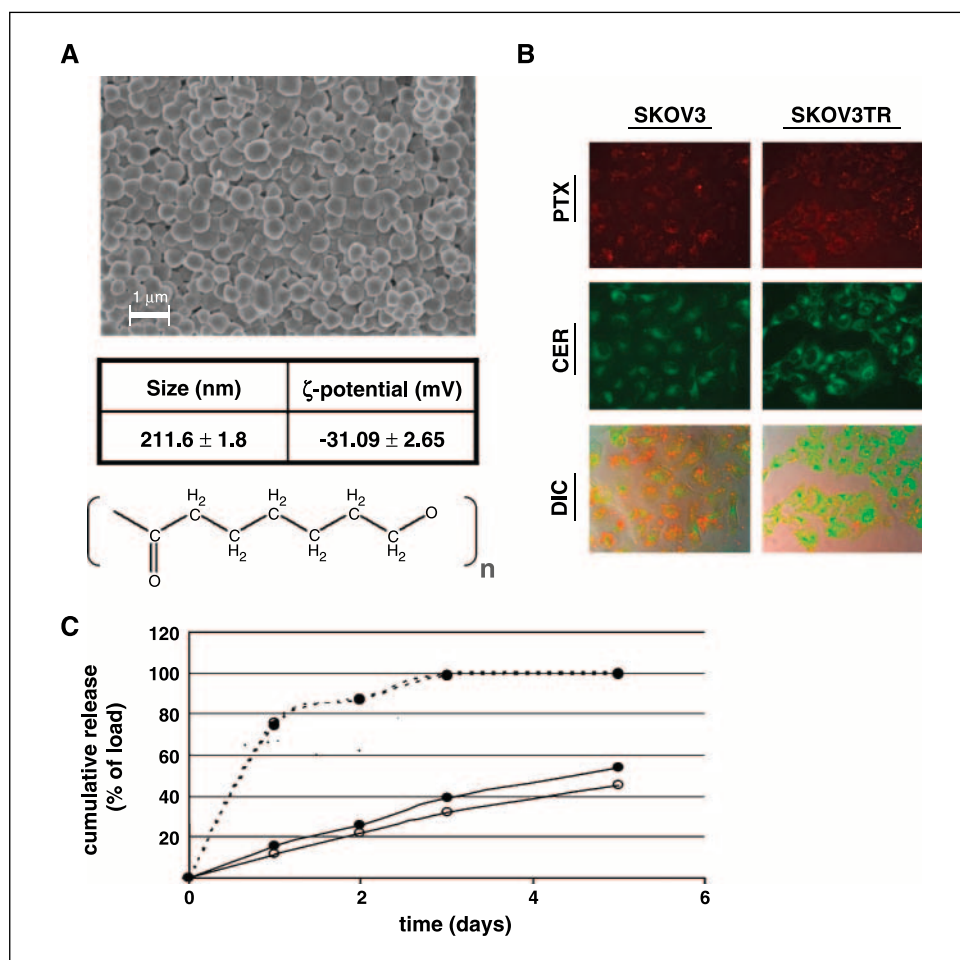
## Results

Production of PEO-PCL nanoparticles resulted in the reproducible formation of spherical particles of uniform size ( $211 \pm 2$  nm), as determined by SEM and dynamic light scattering (Fig. 1A). The particles bear a negative  $\zeta$  potential ( $-31.1$  mV), likely resulting from adsorption of ions from the surrounding medium (Fig. 1A). Although a negative surface charge can challenge nanoparticle endocytosis into cells, visual trafficking of these particles by incorporation of rhodamine-labeled paclitaxel or NBD-labeled ceramide nevertheless revealed that these particles are efficiently taken up into both the drug sensitive (SKOV3) and the MDR (SKOV3TR) cells (Fig. 1B). Drug-loading efficiency into these nanoparticles was 100% for paclitaxel at 10% (w/w) and 70% for ceramide at 20% (w/w), and release studies revealed a complete release of ceramide within 3 days, whereas only about half the paclitaxel load was released by day 5 (Fig. 1C), allowing adequate time for nanoparticle accumulation at

the tumor site before release of the majority of the load. Release of both paclitaxel and ceramide did not seem to be affected by pH, in which similar release was seen at pH 7.4 (physiologic pH) as well as at pH 6.5 (tumor environment).

Preliminary studies on the SKOV3 and its MDR subculture SKOV3TR revealed that the MDR cells abundantly express GCS and the classic MDR marker P-glycoprotein, in contrast to the drug-sensitive SKOV3 cells (Fig. 2A) verifying the MDR phenotype. Concomitantly, dose-response studies against paclitaxel revealed that the SKOV3TR line is at least 100-fold more resistant to paclitaxel than its drug-sensitive counterpart as seen by the far right-shifted dose-response curve (Fig. 2B). The experimental  $IC_{50}$  for the SKOV3 cells was set at  $\sim 0.0084$   $\mu\text{mol/L}$ , whereas the  $IC_{50}$  for the MDR subculture (SKOV3TR) was set over 100-fold higher at 1.08  $\mu\text{mol/L}$ . To verify the therapeutic use of  $C_6$ -ceramide over other ceramide analogues, a variety of ceramide analogues differing in carbon chain lengths ( $C_2$ ,  $C_6$ ,  $C_{10}$ ,  $C_{14}$ ,  $C_{18}$ , and  $C_{24}$ ) were tested side by side on the MDR cell line at equal doses of 15  $\mu\text{mol/L}$ . Results revealed that, coinciding with other scientific reports, the  $C_6$ -ceramide analogue had the most cytotoxic potential (at  $52.4 \pm 3.3\%$  cell death) and were, thus, deemed the most appropriate therapeutic (Fig. 2C). It is important to note that the ceramide analogues were delivered to the cells packaged within PEO-PCL nanoparticles at 20% (w/w) to standardize internalization of the ceramide analogues into the cells. However, equivalent studies were

**Figure 1.** Characterization of PEO-PCL nanoparticles. A, SEM image at 13,000 $\times$  magnification (top), size and  $\zeta$ -potential of nanoparticles (representative from three batches; middle), and chemical structure of PCL (bottom). B, intracellular uptake of rhodamine-paclitaxel (PTX; red) and NBD-ceramide (CER; green) loaded PEO-PCL nanoparticles in SKOV3 (top row) and SKOV3TR cells (bottom row) at 6 h incubation. Differential interference contrast (DIC) shown as merged image with fluorescence. C, drug release from nanoparticles over time of paclitaxel (solid line) and ceramide (dashed line) at pH 7.4 (closed circles) and pH 6.5 (open circles).



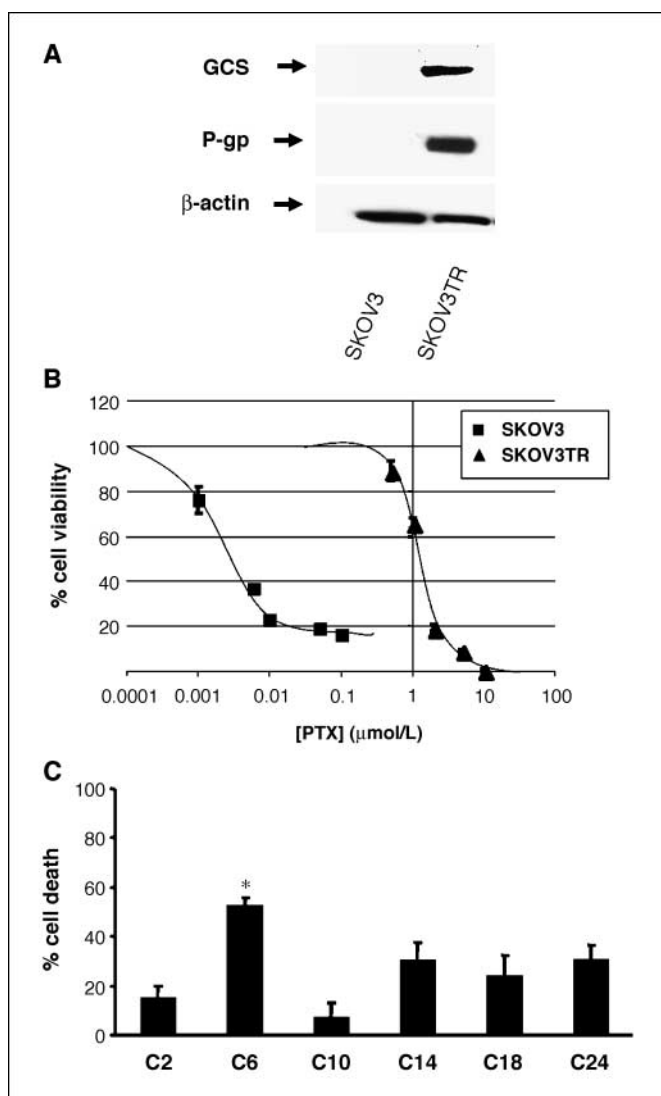


**Figure 2.** Characterization of drug resistant phenotype of SKOV3<sub>TR</sub> cells. **A**, Western blot analysis of P-glycoprotein and GCS expression as a marker for MDR.  $\beta$ -Actin serves as an internal control. **B**, dose-response relationship of drug-sensitive SKOV3 and MDR SKOV3<sub>TR</sub> cells to paclitaxel ( $n = 8$  samples per treatment). **C**, cytotoxicity profile of the various synthetic ceramide analogues at a dose of 15  $\mu\text{mol/L}$ . \*,  $P < 0.05$  of C<sub>6</sub> from the other ceramide analogues.

done in parallel, whereby the ceramide analogues were delivered to the cells as free drug in solution, revealing that even then the C<sub>6</sub> analogue had the most cytotoxic potential (results not shown).

To determine then whether the proposed paclitaxel-ceramide cotherapy indeed possessed the ability to overcome MDR, both the SKOV3 and SKOV3<sub>TR</sub> cells were subjected to treatments with the cotherapy alongside appropriate controls. Because paclitaxel is a cell-cycle specific chemotherapeutic drug, treatments were allowed to proceed undisturbed for 6 days to ensure that all cells initiated mitosis. However, to minimize uncontrolled growth of the cell population in control samples due to the extended treatment duration, all cell samples were seeded near confluency.

Counts of remaining cell viability after treatment revealed that exposure to paclitaxel in combination with ceramide indeed significantly increased the amount of cell death in the MDR population. Figure 3A depicts how the ceramide cotherapy greatly reduced chemoresistance of the MDR ovarian cancer cells

(SKOV3<sub>TR</sub>) when the therapy was given as free drugs in the solution. Treatment of the SKOV3<sub>TR</sub> cells with 10  $\mu\text{mol/L}$  C<sub>6</sub>-ceramide in combination with paclitaxel around IC<sub>50</sub> (1  $\mu\text{mol/L}$ ) improved chemosensitivity of these cells to near complete cell death ( $97.3 \pm 0.5\%$ ,  $P < 0.001$  versus paclitaxel treatment alone at 1  $\mu\text{mol/L}$ ), a profile similar to the chemosensitization seen with the P-glycoprotein inhibitor and first generation MDR modulator verapamil at the same dose ( $93.4 \pm 0.8\%$  cell death at 1  $\mu\text{mol/L}$  paclitaxel and 10  $\mu\text{mol/L}$  verapamil,  $P < 0.001$  versus paclitaxel treatment alone at 1  $\mu\text{mol/L}$ ). Interestingly, the concentration of ceramide used alongside paclitaxel was below the minimal effective concentration for ceramide. For comparison, tamoxifen, a reported inhibitor of GCS (28), was also dosed alongside paclitaxel to test the assumption that an increase in intracellular ceramide, either accomplished by exogenous administration or by inhibition of ceramide metabolism through GCS, is needed to revert chemoresistance of the MDR cancer phenotype. And indeed,

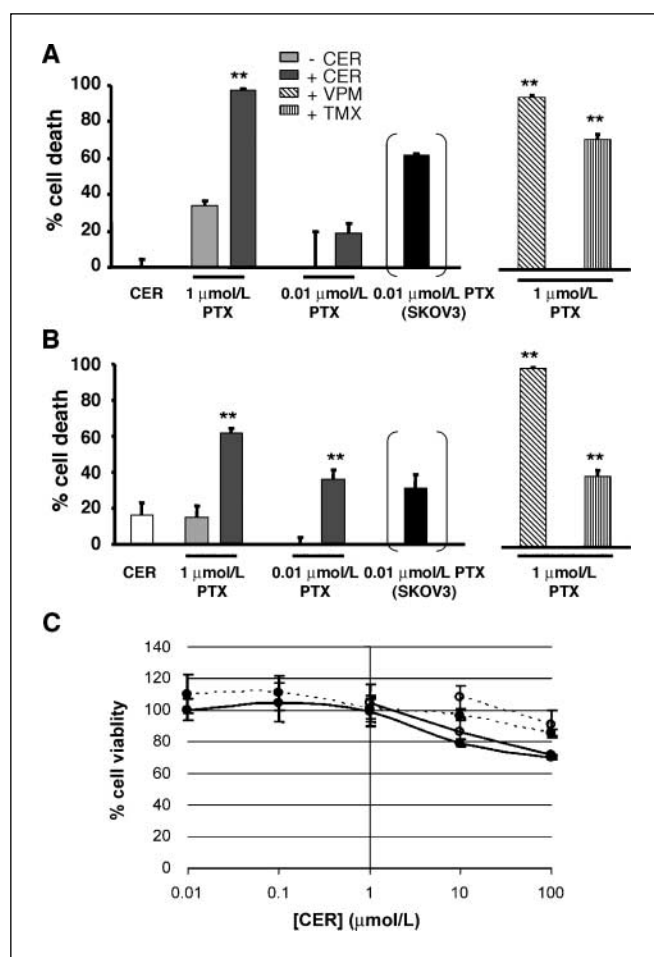
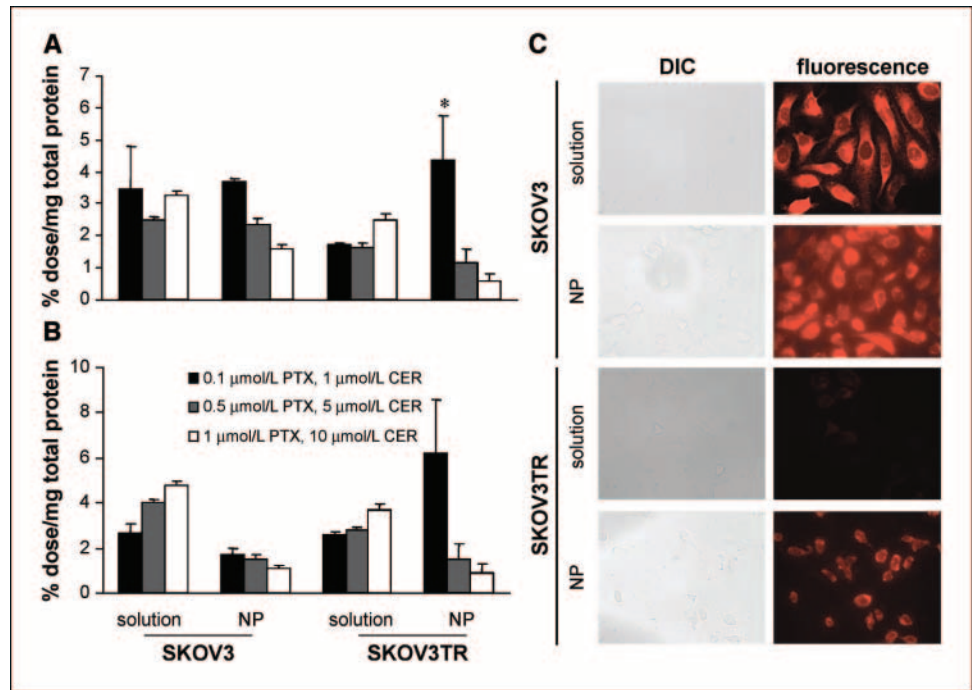


**Figure 3.** Cell kill efficacy of the paclitaxel-ceramide cotreatment on the MDR cell type (SKOV3<sub>TR</sub>), in which the treatments are given (**A**) as free drugs in solution and (**B**) encapsulated in PEO-PCL nanoparticles. Controls include treatment with ceramide alone at 10  $\mu\text{mol/L}$  (the dose given alongside paclitaxel), treatment with verapamil (VPM; 10  $\mu\text{mol/L}$ ) in combination with paclitaxel, and treatment with tamoxifen (TMX; 15  $\mu\text{mol/L}$ ) in combination with paclitaxel. Cell kill efficacies of 0.01  $\mu\text{mol/L}$  paclitaxel on the drug-sensitive SKOV3 cells (*in brackets*). **C**, cell kill efficacy of ceramide treatment on AML-12 cells treated with ceramide (*closed circles*) alongside its vehicle (*open circles*) in solution (*solid line*) or in nanoparticles (*dashed line*). \*\*,  $P < 0.001$  between the cotreatment and paclitaxel alone at a given dose of paclitaxel ( $n = 8$  samples per treatment).

**Figure 4.** Dose-dependent intracellular accumulation of (A) [ $^3\text{H}$ ]paclitaxel and (B) [ $^{14}\text{C}$ ]ceramide delivered as free drugs in solution or encapsulated in PEO-PCL nanoparticles (NP) after 6 h of treatment. C, intracellular retention of rhodamine-123 4 h after administration under  $40\times$  magnification and 400 ms exposure ( $n = 3$  samples per group per cell type).

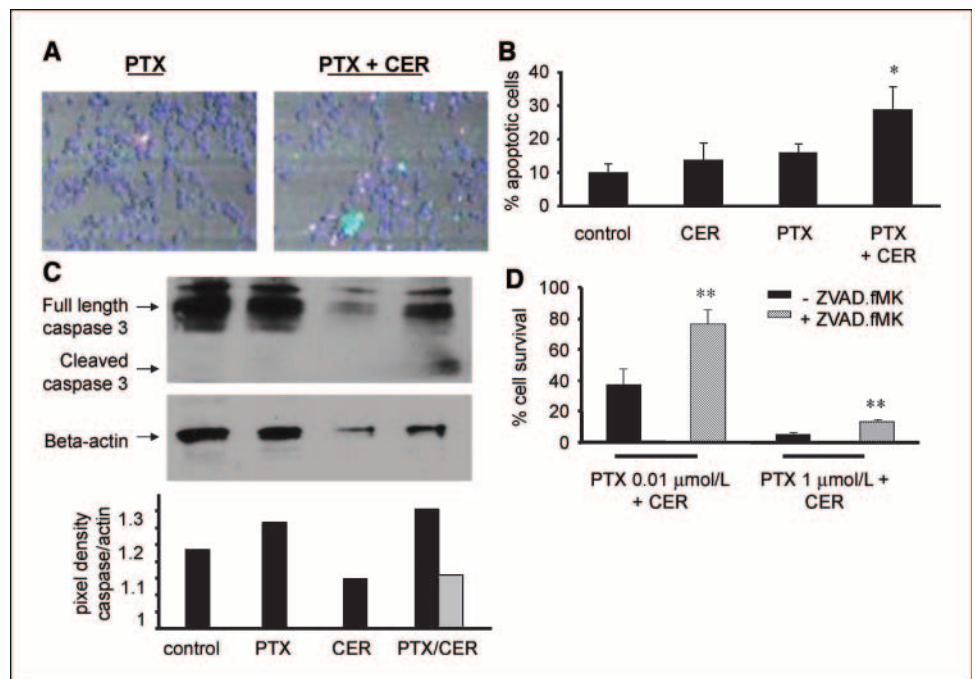


treatment with  $1 \mu\text{mol/L}$  paclitaxel plus  $15 \mu\text{mol/L}$  tamoxifen also significantly increased the amount of resultant cell death to  $70.4 \pm 2.8\%$  (from  $34.4 \pm 2.2\%$  cell death with paclitaxel alone at  $1 \mu\text{mol/L}$ ). Note that, the SKOV3 and SKOV3TR cell lines are estrogen-negative, indicating that their growth is not inhibited by the antiestrogen therapeutic action of tamoxifen (31).

Although the combination of paclitaxel with ceramide in itself caused a significant increase in resultant cell death of the MDR cells, the therapy as is did not have the power to chemosensitize at

lower doses of paclitaxel, particularly in the range in which the drug sensitive cells do respond. For example, treatment of the MDR cells with  $0.01 \mu\text{mol/L}$  paclitaxel (near  $\text{IC}_{50}$  of the drug sensitive SKOV3 cells) with  $10 \mu\text{mol/L}$  ceramide did not significantly improve the amount of cell death over treatment with  $0.01 \mu\text{mol/L}$  paclitaxel alone when these therapeutics were given as free drugs (Fig. 3A). Although the use of a nanoparticle delivery system is mostly for the *in vivo* benefit of improved tumor-specific drug accumulation, the potential for this ceramide

**Figure 5.** Increase in apoptotic activity resulting from paclitaxel-ceramide cotreatment (24 h) in SKOV3TR cells, exposed to  $1 \mu\text{mol/L}$  paclitaxel  $\pm$   $10 \mu\text{mol/L}$  ceramide, alongside  $10 \mu\text{mol/L}$  ceramide alone or control (no treatment). Fluorescent microscopy indicates (A) an increase in apoptotic staining (red/green) in cells treated with paclitaxel and ceramide compared with paclitaxel treatment alone and (B) simultaneous quantitation of apoptotic activity by liquid scintillation counter. C, Western blot analysis of full-length (black columns) and cleaved (gray columns) caspase-3 expression in the treatment groups. D, percentage cell survival with and without coadministration of the pan-caspase inhibitor ZVAD.fmk at doses of  $0.01 \mu\text{mol/L}$  paclitaxel +  $10 \mu\text{mol/L}$  ceramide and  $1 \mu\text{mol/L}$  paclitaxel +  $10 \mu\text{mol/L}$  ceramide. \*,  $P < 0.05$  between paclitaxel + ceramide and paclitaxel or control ( $n = 6$  samples per treatment per cell type). \*\*,  $P < 0.001$  between ZVAD supplemented treatments and nonsupplemented treatments at the same doses ( $n = 8$  samples per group).



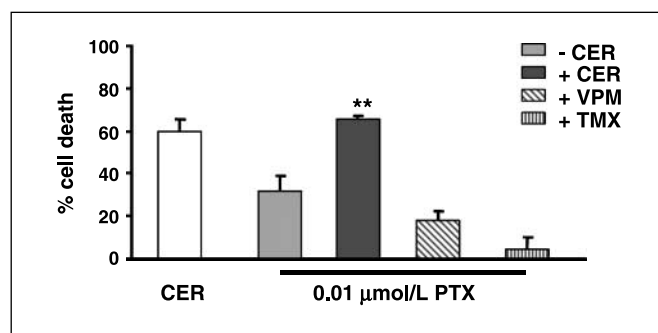


**Figure 6.** Cell kill efficacy of the PEO-PCL nanoparticulate paclitaxel-ceramide cotreatment on the drug sensitive cell type (SKOV3), treated with 0.01 μmol/L paclitaxel ± 10 μmol/L ceramide, alongside ceramide alone at 10 μmol/L, 0.01 μmol/L paclitaxel + 10 μmol/L verapamil, and 0.01 μmol/L paclitaxel + 10 μmol/L tamoxifen. \*\*,  $P < 0.001$  between the cotreatment and paclitaxel alone at the given dose of paclitaxel ( $n = 8$  samples per treatment).

cotherapy to overcome MDR improved even further when the therapeutics were encapsulated and delivered within PEO-PCL nanoparticles. Figure 3B shows that in this mechanism, treatment again with 10 μmol/L ceramide alongside 0.01 μmol/L paclitaxel now resulted in  $36.0 \pm 5.0\%$  cell death, a significant enhancement over the lack of cell death with 0.01 μmol/L paclitaxel alone ( $P < 0.001$ ). It is important to note that blank (unloaded) nanoparticles were given to the cells as a control to show that the nanoparticle matrix itself or its degradation products does not cause any cytotoxicity ( $103.5 \pm 4.6\%$  and  $95.2 \pm 3.7\%$  cell viability in the SKOV3<sub>TR</sub> and SKOV3 lines, respectively). The result with nanoparticle administration of the cotherapeutics is particularly striking because this profile mimics the amount of cell death seen in the drug-sensitive SKOV3 cells ( $31.3 \pm 7.3\%$ ) at 0.01 μmol/L paclitaxel. On the other spectrum, the higher dose (1 μmol/L) of paclitaxel and paclitaxel-ceramide results overall in a lower amount of cell death with the nanoparticle therapy (Fig. 3B) versus the unencapsulated therapy (Fig. 3A). The reasoning for this phenomenon is attributable to the fact that nanoparticle uptake into the cell is a saturable process, whereas diffusion of free drug into the cell is not, thereby preventing higher drug doses from entering the cell. Nevertheless, the pattern of MDR modulation remains the same and is even exaggerated at the low dose of paclitaxel.

From previous work by our group, it is known that these PEO-PCL nanoparticles loaded with paclitaxel exhibit nonspecific accumulation mostly within the liver (10), a common site of therapeutic toxicity. To investigate whether ceramide, as a mediator of apoptosis, could potentially act as a cytotoxic agent on normal (nonmalignant) cells upon such nonspecific accumulation, we examined the potency of ceramide on the murine hepatocyte cell line, AML-12. The results in Fig. 3C show that ceramide induces relatively less cell kill (viability,  $79.4 \pm 2.5\%$ ) to the hepatocytes at the therapeutic dose given (10 μmol/L); however, this is only seen in the solution treatment and can be largely attributed to toxicity of the DMSO vehicle (viability,  $86.5 \pm 8.9\%$ ). Ceramide delivered in nanoparticles did not show any toxicity to the cells at this dose (viability,  $96.8 \pm 3.6\%$ ) as the blank nanoparticles did not either (viability,  $108.0 \pm 7.0\%$ ). Similar results were obtained at the 100 μmol/L dose, in which slight cytotoxicity of the drug could potentially be attributed to cell kill by the vehicle. Therefore, the data suggests that the therapeutic dose of ceramide

should not adversely affect liver hepatocytes upon nontarget accumulation. Due to poor solubility and vehicle toxicity, doses above 100 μmol/L could not be given to the cells to determine an  $IC_{50}$  for ceramide to these cells.

Previous work has also shown that drug delivery mediated by these nanoparticles results in an enhanced intracellular drug accumulation profile (32). Figure 4 shows quantitative analysis of [<sup>3</sup>H]paclitaxel and [<sup>14</sup>C]ceramide accumulation, which indicates that nanoparticle delivery causes a significantly greater amount of paclitaxel to accumulate and/or retain in the SKOV3TR cells than when it is given in the solution (Fig. 4A). Because this phenomenon is not seen in the SKOV3 cells as lacking P-glycoprotein, the data suggests that nanoparticle delivery may cause this increase in intracellular drug accumulation in the SKOV3TR cells by sparing the drugs from P-glycoprotein efflux. This presents a potential mechanism to explain the enhanced chemosensitization seen with nanoparticle delivery. This phenomenon, however, leveled off with an increase in dose, mainly due to the fact that nanoparticle uptake to the cells is saturable, hereby also supporting the fact that this enhanced chemosensitization with nanoparticle delivery was only seen at the lower dose of paclitaxel (0.01 μmol/L). This idea is further supported by visualizing intracellular retention and depletion of the fluorophore rhodamine-123, which is a known substrate for the P-glycoprotein transporter (33), after delivery as free compound (solution) or encapsulated within PEO-PCL nanoparticles. The results in Fig. 4C show that whereas rhodamine-123 is efficiently retained in the SKOV3 cells as lacking P-glycoprotein, 4 h after administration of the compound either in the solution or in nanoparticles, the fluorophore is no longer detectable at this time point within the SKOV3<sub>TR</sub> cells when rhodamine-123 is given as solution. Strikingly, although the rhodamine-123 that was encapsulated within the nanoparticles was retained to a greater extent in the SKOV3TR cells, suggesting that intracellular nanoparticle delivery may indeed help avoid P-glycoprotein efflux of the drugs. The paclitaxel-ceramide nanoparticle therapy revealed a potential to resensitize the MDR cancer cells nearly 100-fold, an effect that could be attributed by a synergistic modulation of ceramide metabolism and P-glycoprotein efflux, although further research is under way to fully explore this mechanism.

It is hypothesized that feedback of exogenous ceramide to MDR cells restores the blocked apoptotic signal initiated by chemotherapeutic stress, because in these cells endogenous ceramide is metabolized to a defunct apoptotic mediator, glucosylceramide. To confirm that this experimental therapy indeed overcomes MDR by mending alterations in the apoptotic signaling cascade, apoptotic activity was measured 24 h after treatment initiation by microplate cytometry and confirmed by simultaneous fluorescent microscopy, maintaining the same conditions set forth in the cytotoxicity studies. Figure 5A indicates that MDR cells exposed to the paclitaxel-ceramide cotreatment at a dose around the SKOV3TR  $IC_{50}$  for paclitaxel (1 μmol/L paclitaxel + 10 μmol/L ceramide) displayed an increased amount of apoptotic staining where the green fluorescent dye YO-PRO-1 stains apoptotic cells and the red fluorescent propidium iodide stains necrotic cells (and dead cells) based on their ability to permeate the cell membrane. Given the recent observations of apoptotic cell death mechanisms that portray a necrosis-like morphology, in which ceramide is thought to play an important role (34–36), the sum of green and red fluorescence was counted toward apoptotic activity but with cytometry gating set to quantify only whole cells (thereby excluding dead cells and cell fragments). The quantitative result revealed that

apoptotic activity in the MDR cells in response to paclitaxel-ceramide treatment is indeed doubled over paclitaxel treatment alone ( $29.0 \pm 3.1\%$  with paclitaxel-ceramide versus  $15.9 \pm 1.9\%$  paclitaxel alone,  $P < 0.05$ ; Fig. 5B). Analysis of the activity of the downstream effector caspase, caspase-3, by Western blotting after a 24-h treatment period with  $1 \mu\text{mol/L}$  paclitaxel and  $10 \mu\text{mol/L}$  ceramide revealed that paclitaxel-ceramide cotreatment caused cleavage of full-length caspase-3 (37 kDa) to its 19 and 17 kDa fragments (Fig. 5C), verifying that the paclitaxel-ceramide cotreatment indeed restores apoptotic signaling in the MDR cells. To determine whether this restored apoptotic activity is via caspase-dependent mechanisms or via the recently hypothesized caspase-independent mechanisms that ceramide seems involved in (34–36), the MDR cells were again subjected to the paclitaxel-ceramide treatment, this time with or without the pan-caspase inhibitor ZVAD.fMK. Cell survival analysis after the 6-day treatment revealed that ZVAD.fMK indeed inhibited a fraction of cell death resultant from the paclitaxel-ceramide cotherapy, in which inhibition was greater when the chemotherapeutic stress was less ( $76.6 \pm 8.9\%$  cell survival with ZVAD.fMK versus  $37.4 \pm 9.7\%$  cell survival without ZVAD.fMK at a dose of  $0.01 \mu\text{mol/L}$  paclitaxel +  $10 \mu\text{mol/L}$  ceramide,  $P < 0.001$ ; Fig. 5D). However, caspase blockade inhibited cell death merely partially, rather than fully, suggesting an involvement of both caspase-dependent and caspase-independent mechanisms of apoptosis in the restoration of apoptotic signal by this novel therapy.

Lastly, it is important to note that, unlike first generation MDR modulation therapies via P-glycoprotein inhibitors, such as verapamil and cyclosporine-A, this novel nanoparticulate paclitaxel-ceramide cotherapy has the potential to chemosensitize drug sensitive cancer cells as well. Subjecting the drug-sensitive SKOV3 cells to the same therapy shown effective on the MDR cells, namely  $0.01 \mu\text{mol/L}$  paclitaxel +  $10 \mu\text{mol/L}$  ceramide in PEO-PCL nanoparticles, doubles the percentage of cell death of the drug sensitive population ( $65.6 \pm 1.1\%$  with paclitaxel-ceramide versus  $31.3 \pm 7\%$  with paclitaxel alone,  $P < 0.001$ ; Fig. 6). However, unlike the MDR cells, this accompanying dose of ceramide is quite cytotoxic to the SKOV3 cells ( $59.5 \pm 5.9\%$  cell death). Nevertheless, these results indicate that this novel therapy would allow for a low dose of paclitaxel to not only eradicate the population of cells in the tumor that have developed MDR but also enhance the therapeutic efficacy of paclitaxel therapy on the subset of cells in the tumor that may have retained drug sensitivity. This effect is in sound contrast to the efficacy of other MDR modulation therapies on drug sensitive cells, which merely enhance chemosensitivity of MDR cells. Figure 6 shows how treatment with the P-glycoprotein inhibitor verapamil or the GCS inhibitor tamoxifen, alongside paclitaxel, does not raise chemotherapeutic efficacy in these drug-sensitive cells over treatment with paclitaxel alone.

## Discussion

The development of the MDR phenotype is a major hurdle for successful treatment of cancer, whereby patients with MDR tumor types are often left with few options but exceptionally high doses or combinations of chemotherapeutics. Paclitaxel, a chemotherapeutic commonly used in the treatment of breast and ovarian tumors, is known to exert its antitumor effect by promoting programmed cell death (apoptosis) in response to its action as a mitotic spindle poison (37). Of interest was the recent observation that paclitaxel cytotoxicity may provoke an intracellular accumulation of endog-

enous ceramide, a lipid that is known to function as a second messenger in the apoptotic signaling cascade. Combining these facts with the latest observations that MDR cells have increased levels of GCS, the enzyme responsible for bioactivation of ceramide, and glucosylceramide, the apoptotically defunct metabolite of ceramide, led to the hypothesis that MDR may be reversed by coadministration of exogenous ceramide with a chemotherapeutic, paclitaxel in this model, to reinstate the apoptotic signaling cascade and resensitize the cancer cells to paclitaxel chemotherapy. To enhance overall efficacy of the therapy, the drugs were encapsulated and delivered to the cells within PEO-PCL nanoparticles.

The results of this study indicate that the combination of paclitaxel-ceramide therapy can indeed greatly improve chemosensitivity of MDR ovarian cancer cells, showed when simply coadministering ceramide with paclitaxel near the paclitaxel  $\text{IC}_{50}$  ( $1 \mu\text{mol/L}$ ) for these cells tripled the percentage cell death in the population. However, the power of this cotherapy to modulate MDR at low doses of paclitaxel (near the paclitaxel  $\text{IC}_{50}$  for the drug sensitive cells) failed, potentially due to residual drug-efflux mediated by P-glycoprotein. It was, therefore, not surprising that delivery of the cotherapeutics within PEO-PCL nanoparticles seemed to overcome these limitations and sensitize the MDR cells to the same doses of paclitaxel at which the drug-sensitive cells were susceptible. Both quantitative and qualitative data indicated that nanoparticle delivery increased intracellular retention of the drug-load in the MDR cells, supporting the possibility that nanoparticle drug delivery could help bypass P-glycoprotein drug efflux, a second common mechanism of MDR.

Because this therapeutic strategy primarily aims at restoring apoptotic signaling to overcome MDR, it was important to illustrate that signaling is indeed improved in cells treated with this novel therapy. Analysis of apoptotic activity indicated that the combination of paclitaxel-ceramide doubled the amount of apoptotic cells in the MDR population over treatment with paclitaxel or ceramide alone. Furthermore, Western blot analysis of the main effector caspase, caspase-3, also suggested this increase in apoptotic activity through the presence of caspase cleavage products. Given the recent observations that ceramide mediates non-caspase-dependent apoptosis, together with established law that ceramide can mediate caspase-dependent apoptosis, in which it acts on mitochondrial dysfunction (38, 39), the question arose whether this restoration of apoptotic signaling in the MDR population proceeded via caspase-dependent or caspase-independent mechanisms. Interestingly, it was found that caspase inhibition was able to reverse a fraction of cell death from to the paclitaxel-ceramide treatment, although not fully, suggesting that the exogenously given ceramide may function in activating both mechanisms of programmed cell death.

Nevertheless, the results of this study portray a beneficial therapeutic strategy for reversing MDR in cancer by a novel approach that targets multiple cellular mechanisms that give rise to MDR. Furthermore, unlike many prior therapeutic strategies to overcome MDR, this novel paclitaxel-ceramide nanoparticle therapy also shows great potential for use in the treatment of non-MDR cancer types, in which therapeutic efficacy of paclitaxel is also enhanced. Ongoing studies are further investigating the therapeutic efficacy of this novel treatment in an *in vivo* model of MDR cancer and are also elaborating on the potential of this ceramide modulation therapy to resensitize a variety of MDR tumor types to an assortment of chemotherapeutic approaches. However, the benefit of overcoming paclitaxel resistance in

ovarian cancer weighs heavily given the clinical relevance, and these results show a promising clinical potential for this therapeutic strategy to increase chemotherapeutic efficacy and overcome such MDR.

## Acknowledgments

Received 5/9/2006; revised 1/24/2007; accepted 2/27/2007.

## References

- Bradley G, Juranka PF, Ling V. Mechanism of multidrug resistance. *Biochem Biophys Acta* 1988;948: 87–128.
- Goldstein LJ, Galski H, Fojo A, et al. Expression of a multidrug resistance gene in human cancers. *J Natl Cancer Inst* 1989;81:116–24.
- Harris AL, Hochhauser D. Mechanisms of multidrug resistance in cancer treatment. *Acta Oncol* 1992;31:205–13.
- Chawla JS, Amiji MM. Biodegradable poly(epsilon-caprolactone) nanoparticles for tumor-targeted delivery of tamoxifen. *Int J Pharm* 2002;249:127–38.
- Chawla JS, Amiji MM. Cellular uptake and concentrations of Tamoxifen upon administration in poly(epsilon-caprolactone) nanoparticles. *AAPS Pharmsci* 2003;5: article 1.
- Woodward SC, Brewer PS, Moatamed R, Schindler A, Pitt CG. The intracellular degradation of poly(epsilon-caprolactone) nanoparticles. *J Biomed Mater Res* 1985; 19:437–44.
- Pitt CG, Gratzl M, Kimmel GL, Surlis J, Schindler A. Aliphatic polyesters II. The degradation of poly(DL-lactide), poly(epsilon-caprolactone), and their copolymers *in vivo*. *Biomaterials* 1981;2:215–20.
- Serrano MC, Pagani R, Vallet-Regi M, et al. *In vitro* biocompatibility assessment of poly(epsilon-caprolactone) films using L929 mouse fibroblasts. *Biomaterials* 2004;25:5603–11.
- Uhrich KE, Cannizzaro SM, Langer RS, Shakesheff KM. Polymeric systems for controlled drug release. *Chem Rev* 1999;99:3181–98.
- Shenoy DB, Amiji MM. Poly(ethylene oxide)-modified poly(epsilon-caprolactone) nanoparticles for targeted delivery of tamoxifen in breast cancer. *Int J Pharm* 2005; 293:261–70.
- Ferrari M. Cancer nanotechnology: opportunities and challenges. *Nat Rev Cancer* 2005;5:161–71.
- Shenoy D, Little S, Langer R, Amiji M. Poly(ethylene oxide)-modified poly(beta amino ester) nanoparticles as a pH sensitive system for tumor-targeted delivery of hydrophobic drugs: part 2. *In vivo* distribution and tumor localization studies. *Pharm Res* 2005;22:2107–14.
- Wani MC, Taylor HL, Wall ME, Coggon P, McPhail AT. Plant antitumor agents: VI. The isolation and structure of taxol, a novel antitumor and antileukemic agent from *Taxus brevifolia*. *J Am Chem Soc* 1971;18:242–60.
- Khayat D, Antoine EC, Coeffic D. Taxol in the management of cancers of the breast and the ovary. *Cancer Invest* 2000;18:242–60.
- Bhalla KN. Microtubule-targeted anticancer agents and apoptosis. *Oncogene* 2003;22:9075–86.
- Vikhanskaya F, Vignati S, Beccaglia P, et al. Inactivation of p53 in a human ovarian cancer cell line increases the sensitivity to paclitaxel by inducing G<sub>2</sub>-M arrest and apoptosis. *Exp Cell Res* 1998;241:96–101.
- Charles AG, Han TY, Liu YY, Hansen N, Giuliano AE, Cabot MC. Taxol-induced ceramide generation and apoptosis in human breast cancer cells. *Cancer Chemother Pharmacol* 2001;47:444–50.
- Senchenkov A, Litvak DA, Cabot MC. Targeting ceramide metabolism - a strategy for overcoming drug resistance. *J Nat Cancer Inst* 2001;93:347–57.
- Kolesnick R. The therapeutic potential of modulating the ceramide/sphingomyelin pathway. *J Clin Invest* 2002;110:3–8.
- Sietsma H, Veldman RJ, Kok JW. The involvement of sphingolipids in multidrug resistance. *J Membr Biol* 2001;181:153–162.
- Selzner M, Bielawska A, Morse MA, et al. Induction of apoptotic cell death and prevention of tumor growth by ceramide analogues in metastatic human colon cancer. *Cancer Res* 2001;61:1233–40.
- Tilly JL, Kolesnick RN. Sphingolipids, apoptosis, cancer treatments and the ovary: investigating a crime against female fertility. *Biochem Biophys Acta* 2002; 1585:135–58.
- Reynolds CP, Maurer BJ, Kolesnick RN. Ceramide synthesis and metabolism as a target for cancer therapy. *Cancer Lett* 2004;206:169–80.
- Radin NS. Killing tumors by ceramide-induced apoptosis: a critique of available drugs. *Biochem J* 2003;371:243–56.
- von Haefen C, Wieder T, Gillissen B, et al. Ceramide induces mitochondrial activation and apoptosis via a Bax-dependant pathway in human carcinoma cells. *Oncogene* 2002;21:4009–19.
- Liu Y-Y, Han T-Y, Giuliano AE, Cabot MC. Ceramide glycosylation potentiates cellular multidrug resistance. *FASEB J* 2001;15:719–30.
- Morjani H, Aouali N, Belhoussine R, Veldman RJ, Levade T, Manfait M. Elevation of glucosylceramide in multidrug-resistant cancer cells and accumulation in cytoplasmic droplets. *Int J Cancer* 2001;94:157–65.
- Lavie Y, Cao H, Volner A, et al. Agents that reverse multidrug resistance, tamoxifen, verapamil, and cyclosporin A, block glycosphingolipid metabolism by inhibiting ceramide glycosylation in human cancer cells. *J Biol Chem* 1997;272:1682–7.
- Lucci A, Cho WI, Han TY, Giuliano AE, Morton DL, Cabot MC. Glucosylceramide: a marker for multiple-drug resistant cancers. *Anticancer Res* 1998; 18:475–80.
- Itoh M, Kitano T, Watanabe M, et al. Possible role of ceramide as an indicator of chemoresistance: decrease of the ceramide content via activation of glucosylceramide synthase and sphingomyelin synthase in chemoresistant leukemia. *Clin Cancer Res* 2003;9:415–23.
- Hua W, Christianson T, Rougeot C, Rochefort H, Clinton GM. SKOV3 ovarian carcinoma cells have functional estrogen receptor but are growth-resistant to estrogen and antiestrogens. *J Steroid Biochem Mol Biol* 1995;55:279–89.
- Shenoy D, Little S, Langer R, Amiji M. Poly(ethylene oxide)-modified poly(beta amino ester) nanoparticles as a pH-sensitive system for tumor-targeted delivery of hydrophobic drugs: Part I. *In vitro* evaluations. *Mol Pharm* 2005;2:357–66.
- Wang Y, Hao D, Stein WD, Yang L. A kinetic study of Rhodamine-123 pumping by P-glycoprotein. *Biochem Biophys Acta* 2006;1758:1671–6.
- Thon L, Mohlig H, Mathieu S, et al. Ceramide mediates caspase-independent programmed cell death. *FASEB J* 2005;19:1945–56.
- Granot T, Milhas D, Carpentier S, et al. Caspase-dependent and -independent cell death of Jurkat human leukemia cells induced by novel synthetic ceramide analogs. *Leukemia* 2006;20:392–9.
- Kim WH, Choi CH, Kang SK, Kwon CH, Kim YK. Ceramide induces non-apoptotic cell death in human glioma cells. *Neurochem Res* 2005;30:969–79.
- Ganasia-Leymarie V, Bischoff P, Bergerat JP, Holl V. Signal transduction pathways of taxanes-induced apoptosis. *Curr Med Chem Anti-Canc Agents* 2003;3: 291–306.
- Siskind LJ. Mitochondrial ceramide and the induction of apoptosis. *J Bioeng Biomembr* 2005;37:143–53.
- Jacotot E, Costantini P, Laboureaux E, Zamzami N, Susin SA, Kroemer G. Mitochondrial membrane permeabilization during the apoptotic process. *Ann N Y Acad Sci* 1999;887:18–30.